

Thermoelectric Energy Harvesting in Aircraft

Th. Becker (Airbus Group Innovations), A. Elefsiniotis (Airbus Group Innovations), M. E. Kiziroglou (Imperial College London)

1. Introduction

Energy harvesting is an umbrella term, used to describe methods to generate electrical energy from ambient energy sources. These principles have been explained in detail in the previous chapters, and thermoelectric energy harvesting is reviewed for aeronautical applications in this chapter. Decentralized electrical energy generation from the environment is a key enabler for creating fully autonomous sensor systems or wireless systems in the aeronautic industry. It allows flexible system installation without extensive cabling effort, and improves system modularity in order to enable local system functionalities. Furthermore, it is a maintenance free solution for the perpetual operation of the device to be powered. Last but not least, it allows for rapid provision of new functionalities for retrofits in existing aircraft programs.

With reference to the aviation industry, energy harvesting can potentially provide cost reduction not only for manufacturers, but for the airline companies as well [1], [2]. On one hand, it may decrease production costs by reducing cabling and aircraft customization costs. On the other hand, it offers weight reduction opportunities in case of autonomous wireless sensor networks, compared to entirely wired or wireless data transmission only solutions. In turn, such weight reductions result in lower fuel consumption and operational costs.

The reason for integrating sensor networks in aircraft is to reduce maintenance costs by shifting paradigm from scheduled maintenance to unscheduled or even predictive maintenance. As stated in the previous paragraph, the advantage of wireless and autonomous solutions in terms of weight has been established. Therefore, the wireless sensor technology in general, and more specifically, energy harvesting technology, has been proven as key enabler for aircraft wireless networks such as health monitoring systems.

This chapter begins with a review of aircraft standardization, describing the aircraft environment, followed by an architectural introduction to autonomous wireless sensor nodes and their key features. Next, recently introduced analytical and theoretical models for the thermoelectric harvesting devices are presented in detail. A review of reported thermoelectric harvesting prototypes for aircraft applications is given in section 5. Finally, an outlook of the future of thermoelectric harvesting for aircraft applications is presented in section 6.

2. Aircraft Standardization

The aviation industry has to comply with a lot of specifications and regulations in order to introduce a new technology in aircraft. Additionally, rigorous testing must be conducted, ensuring that any new technology is robust, reliable and safe for in-service use. What is more, aircrafts are divided into fixed-wing and rotary-wing and, of course, in many other sub-categories. Standardization can vary for different aircraft types. However, the purpose of this section is to show the minimum requirements that energy harvesting technologies should fulfill in fixed-wing aircraft in terms of research and technology considerations. A list with the most important standards is presented in

Table 1.

Standard	Title
DO-160G	Environmental Conditions and Test Procedures for Airborne Equipment
DO-167	Airborne Electronics and Electrical Equipment Reliability
DO-171	Recommendations on Policies and Procedures for Off-the-Shelf Electronic Test Equipment Acquisition and Support
DO-178C	Software Considerations in Airborne Systems and Equipment Certification
DO-227	Minimum Operational Performance Standards for Lithium Batteries
DO-254	Design Assurance Guidance for Airborne Electronic Hardware
DO-293A	Minimum Operational Performance Standards for Nickel-Cadmium and Lead Acid Batteries
DO-311	Minimum Operational Performance Standards for Rechargeable Lithium Battery Systems
DO-313	Certification Guidance for Installation of Non-Essential, Non-Required Aircraft Cabin Systems and Equipment
DO-347	Certification Test Guidance for Small and Medium Sized Rechargeable Lithium Batteries and Battery Systems

Table 1: Radio Technical Commission of Aeronautics (RTCA) publishes the standardizations used in aircraft. This table summarizes the most important standards, which need to be fulfilled when introducing a new technology in aircraft.

A description concerning temperature and altitude conditions, temperature variations, humidity and vibrations will be outlined briefly according to the standard DO-160G. In any case, airworthiness has to be proven by complying with all relevant aspects.

The energy harvester might be installed in either a temperature controlled or non-temperature controlled, pressurized or non-pressurized area, respectively. The temperature range for testing energy harvesting devices should be from $-55\text{ }^{\circ}\text{C}$ to $85\text{ }^{\circ}\text{C}$. Pressure tests should be performed from 170 kPa (corresponding to -4.6 km / $-15,000\text{ ft.}$ altitude) to 4.44 kPa (corresponding to 21 km / $70,000\text{ ft.}$ altitude). Temperature variation is not always consistent and therefore specifications should allow for some flexibility. A minimum rate of $2\text{ }^{\circ}\text{C}$ per minute is defined in the standardization (DO-160G).

Another important factor is humidity, which can impact energy harvesting devices in different ways. It can cause corrosion, but it can also influence the physical (e.g. electrical and mechanical) and chemical properties of the device. The energy harvester should be able to withstand harsh temperature and humidity environments, ranging for example, from relative humidity (RH) 85% at 40 °C to 95% RH at 65 °C.

Mechanical vibrations, on the one hand, might be an energy source for a harvester. In this case, the transducer has to be carefully investigated with regard to the expected number of cycles and the calculated lifetime. On the other hand, mechanical vibrations might affect the operational lifetime of a device. Mechanical loads ranging from shock to long lasting vibrations may lead to fatigue on devices. The vibration tests depend strongly on the aircraft type, installation area and test scenario. Due to the huge variety of the resulting test procedures, a simple strategy cannot be suggested. As a consequence, an extensive study on standards should be made before designing and introducing a new technology in aircraft.

3. Autonomous wireless sensor systems

Each autonomous sensor or actuator system, wirelessly connected to a network, requires a very application-specific powering solution. The application-specific requirements have to be analyzed in detail for the design of an energy harvesting device as well as for the wireless sensor node layout. An autonomous sensor or actuator system or wireless sensor node consists typically, as shown in Figure 1, of sensors acquiring the measurement signals or actuators. In addition, it consists of a power supply, in this case the energy harvesting device with an energy storage unit, a power management module with a processor (usually a microcontroller), a data storage medium, and finally, of a transceiver module for communication with a wireless network.

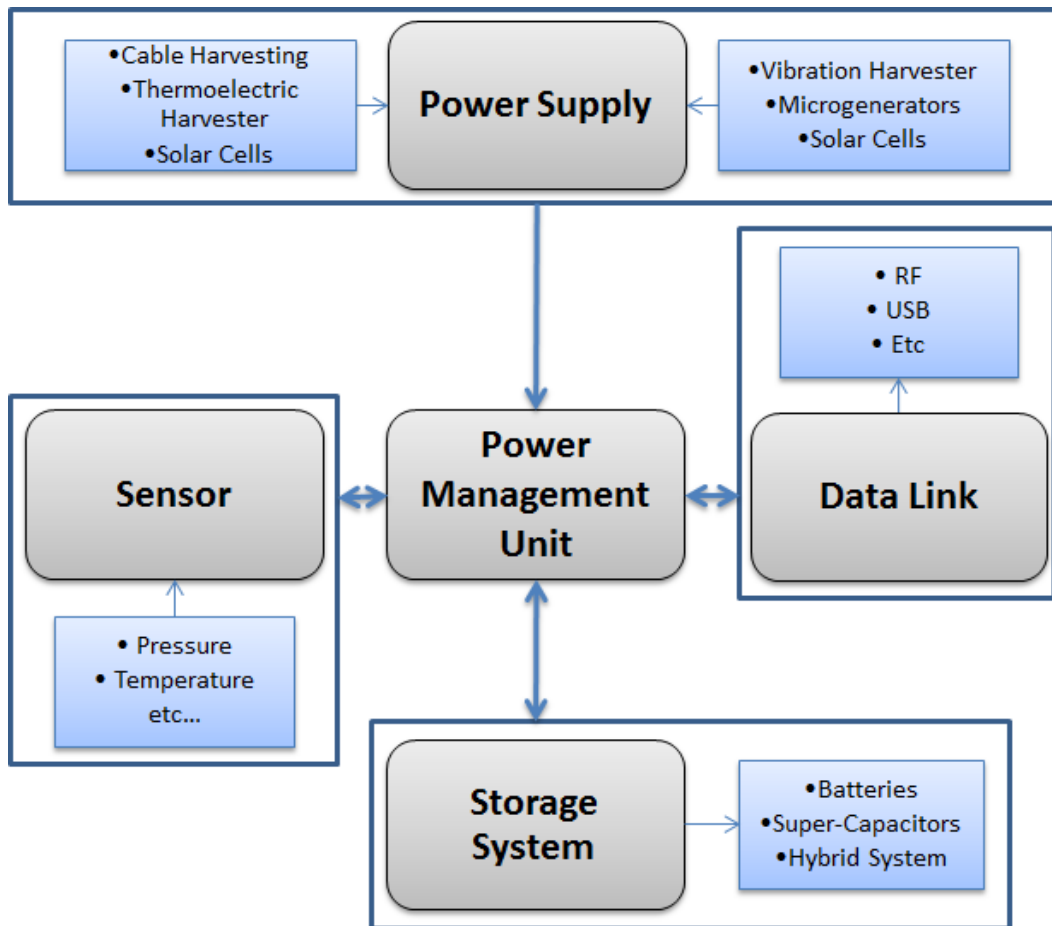


Figure 1: Typical layout of an autonomous sensor (actuator) system or wireless sensor node.

The application scenarios can typically be subdivided into two classes: monitoring tasks and powering small devices. Monitoring tasks are related to the aircraft health assessment so as to decrease maintenance costs. The structural health of an aircraft can be assessed by detecting loads, strain, delamination, de-bonding or cracks. The status of systems and components can be measured with temperature, pressure, humidity or other chemical or physical sensors. The powering of small devices may vary from temporary illumination tasks to small motor operation or to small switches. For a synthesis of an autonomous sensor/actuator system, the selection of the sensor or actuator, the related measurement procedure as well as the operation scheme needs to be analyzed in detail. New sensing technologies and measurement strategies should be used to reduce the power and energy needed.

The environmental conditions a harvesting module experiences, determine its energy output. A study on the possible environmental sources has been conducted [3] and one of the most promising candidates is the many different heat fluxes in aircraft structures. These heat fluxes can be converted into electrical energy by using thermoelectric generators (TEGs), which make use of the Seebeck effect in order to generate electrical power from a temperature difference.

The selection of TEGs should be made very carefully, since their Seebeck coefficient as well as their internal thermal and electrical resistance, determines the design of the power management unit. The Seebeck coefficient determines the open circuit voltage (at a specific ΔT), and plays an important role against the required startup voltage of the power management circuit. In order to maximize the power output, the internal electrical resistance of the TEG should be matched by the equivalent input resistance of the power management. Accordingly, maximum power point tracking (MPPT) algorithms have been developed recently [4]. The power management module is very important for the operation of an autonomous WSN. It is tasked with bringing the output voltages of the harvester to a specified input voltage threshold for a particular load (e.g. sensors, microcontroller etc.). Additionally, it is responsible of storing the surplus electrical energy in a medium (e.g. batteries and/or super-capacitors).

Energy storage is a challenge by itself since batteries and super-capacitors present both advantages and disadvantages. A typical tradeoff is that while batteries have higher energy densities than super-capacitors, super-capacitors have higher power densities [5]. Batteries have a shorter lifetime (number of charging cycles) mainly due to electrode degradation. The runtime is reduced, typically by the internal impedance, the high resistance and other internal losses when batteries are used for storage. In addition, batteries have a relatively limited operational temperature range. Although super-capacitors might be a possible solution, extended periods of downtime are not always possible due to their high self-discharge rate. On the other hand, capacitors typically feature longer lifetimes due to their ability to endure a large number of charging-discharging cycles. Hybrid systems in which batteries and super-capacitors are combined are under research and the advantages are described in detail in [5], [6].

Finally, the wireless sensor node includes the selection of the transceiver and the communication protocol. This part is subject to regulation and certification issues, and the selection of frequencies for communication is e.g. part of the wireless avionics intra-communication project WAIC [7].

4. Thermoelectric energy harvesting in Aircraft

Thermoelectric energy harvesting refers to the conversion of environmental heat flow to electrical energy. A TEG device is typically used for energy transduction through the Seebeck effect. The achievable electrical power depends strongly on the available temperature difference (ΔT) because it determines the heat flow power and also, the TEG conversion efficiency. Thermoelectric generators are solid state devices (no moving parts) which makes them reliable and hence, usable in any location where a temperature difference is present [8]. In the aircraft environment, temperature differences can be found in various locations such as near turbines and other engines or between the interior and exterior during flights. More particularly, such devices can be thermally connected to the inner part of the hull of the aircraft. The aircraft's fuselage serves as an "infinite" thermal energy source. From here on, two approaches to harnessing this energy and creating a heat flux are investigated.

One approach relies on creating a "quasi-static" state, where only passive components like heat pipes and/or heat sinks are used in addition to the TEGs. The heat pipes and heat sinks need to conduct and absorb energy from a higher temperature source like the space between the fuselage and the cabin lining, and conduct it towards and through the TEGs to the fuselage.

The second approach relies on creating a "dynamic" state, where a thermal mass (also referred to in the text as heat storage unit (HSU) is used to temporarily create an artificial temperature difference between the two sides of the TEGs, caused by the significant temperature fluctuation during take-off and landing. By using a thermal mass with great heat capacity on the surface of the TEG not facing the fuselage, the time needed to reach thermal equilibrium is increased, thus increasing electrical energy production. In order to maximize the heat capacity of the thermal mass, a phase change material (PCM) is used. PCMs, when undergoing a phase change, absorb or release energy called latent heat which boosts the amount of energy they can store. However, the phase change temperature is specific to each PCM and somewhat affects their operational temperatures range, making it therefore a crucial factor in device flexibility.

4.1. Efficiency of a thermoelectric energy harvesting device

The thermoelectric phenomena present on a TEG are the Seebeck, Peltier, Thomson and Joule effects. The Thomson effect is neglected in this analysis, and the Joule effect is assumed to be equally distributed between the cold and the hot side [9]. Apart from that, the TEGs are placed between the heat source, in this case the fuselage, and a heat sink (either a heat spreader or a HSU) which introduce a thermal resistance to the system.

The TEG efficiency is defined as electrical output power, P_{el} , over thermal input power \dot{Q}_h ($(I^2 \cdot R_L / \dot{Q}_h)$), with R_L being the resistive load connected to the TEG. Defining the resistance ratio as $\mu = R_L / R_i$, where R_i is internal resistance of the TEG, the following general expression for η_{TEG} can be written [10]:

$$\eta_{TEG} = \frac{\Delta T}{T_h} \cdot \frac{\mu}{(\mu+1)^2 / ZT_h + (\mu+1) - \Delta T / 2T_h} \quad (4.1)$$

The maximum efficiency is obtained when $\mu = \sqrt{1 + ZT_h}$, yielding the usual TEG efficiency expression as derived in Chapter 4 of this book:

$$\eta_{TEG}(\Delta T) = \frac{\Delta T}{T_h} \cdot \frac{\sqrt{1 + ZT} - 1}{\sqrt{1 + ZT} + \frac{T_c}{T_h}} \quad (4.2)$$

This optimum point is different from the maximum power delivery point for a TEG, which is obtained for $\mu = 1$. Physically this means that at maximum power delivery, the TEG allows more heat flow through and overall, it operates less efficiently. In direct (static) thermoelectric harvesting this is not important as an infinite heat flow source can be assumed, so the desirable operation point is $\mu = 1$: maximum power delivery, not maximum TEG conversion efficiency. Nevertheless, in heat storage (dynamic) thermoelectric harvesting, the desirable operation point is theoretically $\mu = \sqrt{1 + ZT_h}$: maximum TEG conversion efficiency at the expense of a lower power delivery. In other words, a slightly greater R_L than R_i is used, reducing the current and thereby partially saving thermal energy for conversion at the maximum overall efficiency. In practice, the low ZT values of state-of-the-art TEGs translate to smaller corresponding efficiency difference (e.g. 6% for $ZT = 1$ at $\Delta T = 30$ °C). Additionally, a slow change in temperature over the harvester, results in more heat leakage through insulation. It is concluded that at least in current TEG technologies, a matching load condition is advisable for characterization and operation of direct or heat storage harvesting. As a result, a more suitable TEG efficiency expression for thermoelectric harvesting applications is that of a matched load condition, i.e. equation 4.1 with $\mu = 1$, as derived in the *thermoelectric maximum power analysis of Chapter 6 of this book*:

$$\eta_{TEG} = \frac{\Delta T}{T_h} \cdot \frac{1}{2 + \frac{4}{ZT_h} - \frac{\Delta T}{2T_h}} \quad (4.3)$$

When ZT_h values are small and high accuracy is not critical, matched load efficiency can be written as:

$$\eta_{TEG} = \frac{Z\Delta T}{4} = \frac{a^2 \Delta T}{4R_e K} = \frac{V_{oc}^2 / 4R_e}{\Delta T / R} \quad (4.4)$$

As expected, the last term of Equation 4.4 is the ratio of load power over heat flow, with the Ohm and Peltier effects still neglected.

4.2. Static thermoelectric energy harvester

The static harvester consists of a TEG with one of its sides attached to a heat source, usually the fuselage. Its other side is attached to a heat spreader or to a heat sink. The basic equations of an ideal thermoelectric harvester then should be modified such that they include the thermal resistances in contact with the TEG. This includes the thermal resistances of the heat source or the fuselage and the heat sink. A schematic of a static harvester with the equivalent thermal and electrical circuits is illustrated in Figure 2.

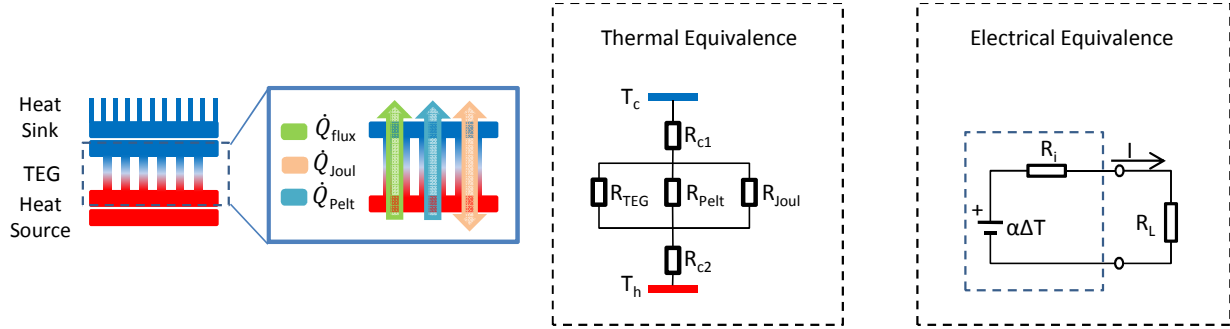


Figure 2: A schematic of a static harvester with the equivalent thermal and electrical circuits.

For the equivalent (lumped) electrical circuit, the current flowing through the load resistance is

$$I = \frac{U}{R} = \frac{\alpha(T)\Delta T_{TEG}}{R_i + R_L} \quad (4.5)$$

where the Seebeck voltage is equal to $U = \alpha(T) \cdot \Delta T_{TEG}$. Consequently, the electrical power output of the equivalent electrical circuit can be written as:

$$P_{el} = U \cdot I = I^2 R_L = \frac{\alpha^2(T)\Delta T_{TEG}^2}{(R_i + R_L)^2} R_L \quad (4.6)$$

where $\Delta T_{TEG} = T_h^{TEG} - T_c^{TEG}$ (as shown in Figure 2). On a static harvester the electrical power output depends on the thermal resistances, since the temperature difference across the TEG is not equal to the temperature difference applied. Using the Fourier heat equation, the heat flow on the cold and on the hot side is equal to [11], [12],

$$q_h = \alpha(T_h)T_h I - \frac{1}{2}I^2 R_i + \frac{\Delta T_{TEG}}{\mathcal{R}_{TEG}} \quad (4.7)$$

$$q_c = \alpha(T_c)T_c I + \frac{1}{2}I^2 R_i + \frac{\Delta T_{TEG}}{\mathcal{R}_{TEG}} \quad (4.8)$$

where \mathcal{R}_{TEG} is the thermal resistance of the TEG. The first term shows the Peltier, the second the Joule and the third the Seebeck effect. The temperature difference which is applied to the system comparing with the temperature difference applied on the TEG can be written as,

$$\Delta T = \Delta T_{TEG} + \mathcal{R}_c q_c + \mathcal{R}_h q_h \quad (4.9)$$

Taking into account only the first order terms of the ΔT_{TEG} as well as a constant Seebeck coefficient for the given temperature range, the temperature difference applied on the TEG, using the Fourier heat equation, can be written as [11],

$$\begin{aligned} \Delta T_{TEG} &= \frac{\Delta T}{1 + \frac{\mathcal{R}_c}{\mathcal{R}_{TEG}} + \frac{\mathcal{R}_h}{\mathcal{R}_{TEG}} + \frac{\alpha^2(T_h)T_h\mathcal{R}_h + \alpha^2(T_c)T_c\mathcal{R}_c}{R_i + L}} \Rightarrow \\ \Delta T_{TEG} &\approx \frac{\Delta T}{1 + (\mathcal{R}_c + \mathcal{R}_h) \left(\frac{1}{\mathcal{R}_{TEG}} + \frac{\alpha^2 T_c}{R_i + R_L} \right)} \end{aligned} \quad (4.10)$$

The last term can be used to determine the power output of a static generator, which by math simplification can be written as [11],

$$P_{el} = (\alpha \Delta T)^2 \left(\frac{\mathcal{R}_{TEG}}{\mathcal{R}_c + \mathcal{R}_h + \mathcal{R}_{TEG}} \right)^2 \frac{R_i}{(R_L + R_i^{eff})^2} \quad (4.11)$$

where the effective internal resistance of the TEG is equal to [11],

$$R_i^{eff} = R_i + \alpha^2 T_c (\mathcal{R}_c + \mathcal{R}_h) \frac{\mathcal{R}_{TEG}}{\mathcal{R}_c + \mathcal{R}_h + \mathcal{R}_{TEG}} \quad (4.12)$$

The maximum power generation of a static harvester can be found by setting $\frac{d}{dR_i} P_{el} \stackrel{\text{def}}{=} 0$ and the result is that the load resistance should match the effective internal resistance.

$$R_L = R_i^{eff} \quad (4.13)$$

If the load resistance is matching the effective internal resistance, and by substituting the figure of merit, $Z = \frac{\alpha \mathcal{R}_{TEG}}{R_i}$ for the power output, the power is maximized when $\frac{d}{d\mathcal{R}_{TEG}} P_{el}(R_L = R_i^{eff}) \stackrel{\text{def}}{=} 0$. This corresponds to a TEG thermal resistance of :

$$\mathcal{R}_{TEG} = (\mathcal{R}_c + \mathcal{R}_h) \sqrt{Z T_c + 1} \quad (4.14)$$

Assuming that the internal electrical resistance is almost equal to the electrical load resistance, the above equation can identify the possible operating ranges. If the internal thermal resistance of the TEG is much smaller than the sum of the hot and cold thermal resistances, the Peltier effect is very big due to the large heat flow. If the internal thermal resistance of the TEG is much greater than the sum of the hot and cold thermal resistances, then the Peltier effect is almost not present due to small heat flow. Nonetheless, the system should be designed in order for the thermal resistance of the TEG to match the sum of the hot and cold thermal resistance of the contacts, achieving the optimal combination of heat flow and ΔT across the TEG.

4.3. Dynamic thermoelectric energy harvester

The operating principle of dynamic thermoelectric harvesting is illustrated in Figure 3. The HSU comprises a PCM inside a container which provides thermal contact to a TEG. The HSU is otherwise thermally insulated from the environment. A uniform temperature distribution inside the HSU is desirable in order to maximize the ΔT across the TEG. For this reason an internal thermal bridge structure is employed which improves the temperature uniformity within the PCM. An insulation layer prevents heat leakage to the environment through the rest of the HSU surface. The outside TEG surface is in thermal contact with the aircraft structure through an appropriate thermally conducting interface. When the aircraft structure temperature fluctuates, heat flows in and out of the HSU through the TEGs, resulting in generation of electrical energy. The energy output of the harvesting device can be collected, stored and distributed by a power management system.

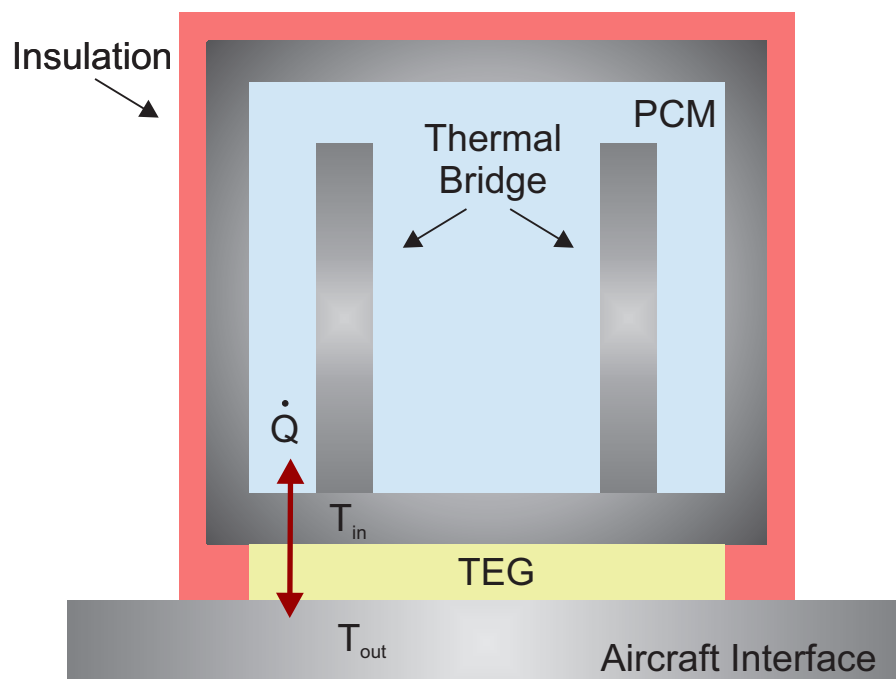


Figure 3: Schematic of the device structure.

The theoretical model for heat storage thermoelectric harvesters is summarized, as originally developed in [13] and [14]. For simplicity, it is assumed that thermal conductivities are independent of temperature. It is also assumed that the PCM has a uniform temperature; temperature gradients in the HSU are negligible and phase change occurs uniformly.

If \mathfrak{R} is the thermal resistance between the environment and a HSU with heat capacity C and latent heat L , then during non-phase change operation, the heat inside the HSU Q and the heat flow \dot{Q} will be:

$$Q = C \cdot T_{in} \quad (4.15)$$

$$\dot{Q} = \frac{\Delta T}{\mathfrak{R}} \quad (4.16)$$

where $\Delta T = T_{out} - T_{in}$ is the difference between outside and inside temperatures. Combining Equation 4.15 with Equation 4.16, one obtains a differential equation for ΔT , for non-phase change operation:

$$\Delta \dot{T} + \frac{\Delta T}{\mathfrak{R}C} = \dot{T}_{out} \quad (4.17)$$

For linear time variation of T_{out} , i.e. $T_{out}(t) = b \cdot t + T_{out}(0)$, an analytical equation for ΔT during non-phase change (NPC) operation can be derived:

$$\Delta T(t)_{NPC} = \Delta T(0) \cdot e^{-\frac{t}{\mathfrak{R}C}} + b \cdot \mathfrak{R}C \cdot (1 - e^{-\frac{t}{\mathfrak{R}C}}) \quad (4.18)$$

The first term on the right side of Equation 4.18 corresponds to the exponentially decaying ΔT that would stem from an initial temperature difference; the second originates from the T_{out} change, and approaches the limit $b \cdot \mathfrak{R}C$ when $t \gg \mathfrak{R}C$. Hence, the value $b \cdot \mathfrak{R}C$ physically represents the constant temperature difference that is established if T_{out} keeps on changing linearly after a time $t \gg \mathfrak{R}C$. As an example, a 1 cm^2 TEG with $\mathfrak{R} = 33 \text{ K/W}$ and 1 cm^3 of water with $C = 4.2 \text{ J/K}$ has an $\mathfrak{R}C = 138 \text{ s}$. At a temperature sweep of $b = 4 \text{ K/min}$, this device would yield a constant $\Delta T = b \cdot \mathfrak{R}C = 9 \text{ K}$ after around 10 min of non-phase change operation.

During phase change operation, T_{in} is constant, and therefore ΔT is the sum of any initial condition $\Delta T(0)$ and the variations in T_{out} :

$$\Delta T(t)_{PC} = b \cdot t + \Delta T(0) \quad (4.19)$$

From the above equations, analytical expressions for heat, heat flow, and HSU temperature can be derived. To find the total electrical energy E_{out} produced by the TEG, heat leakage must be taken into account. If $\delta \cdot \dot{Q}$ is the portion of \dot{Q} that flows through the TEG, then:

$$E_{out} = \int \delta \cdot \dot{Q} \cdot \eta_{TEG} dt = \frac{\delta}{\mathfrak{R}} \int \Delta T(t) \cdot \eta_{TEG} dt \quad (4.20)$$

A formulation for the maximum energy that can be harvested by a heat storage thermoelectric harvester of heat capacity C and latent heat L , from an ambient temperature cycle of change Θ , has been also shown in [13]. The resulting expression is:

$$E_{MAX} = 2 \cdot (\Theta \cdot C + L) \cdot \eta_{TEG} \left(\frac{\Theta}{2} \right) \quad (4.21)$$

where $\eta_{TEG}(\Theta/2)$ is the TEG efficiency at temperature difference $\Delta T = \Theta/2$. This means that the overall maximum efficiency is simply the TEG efficiency for $\Theta/2$. From Equations 4.20 and 4.21 one can calculate the maximum electrical energy per unit mass of heat storage material available from a thermoelectric generator. Indicative simulation results are plotted in Figure 4 as a function of ambient temperature variation, for different TEG figures of merit, using $L/m = 334$ kJ/kg, and $C/m = 4.2$ kJ/(K·kg), where m is the PCM mass. Water was chosen as the PCM because its heat storage properties are superior to other heat storage materials which are typically salt-based or organic solutions.

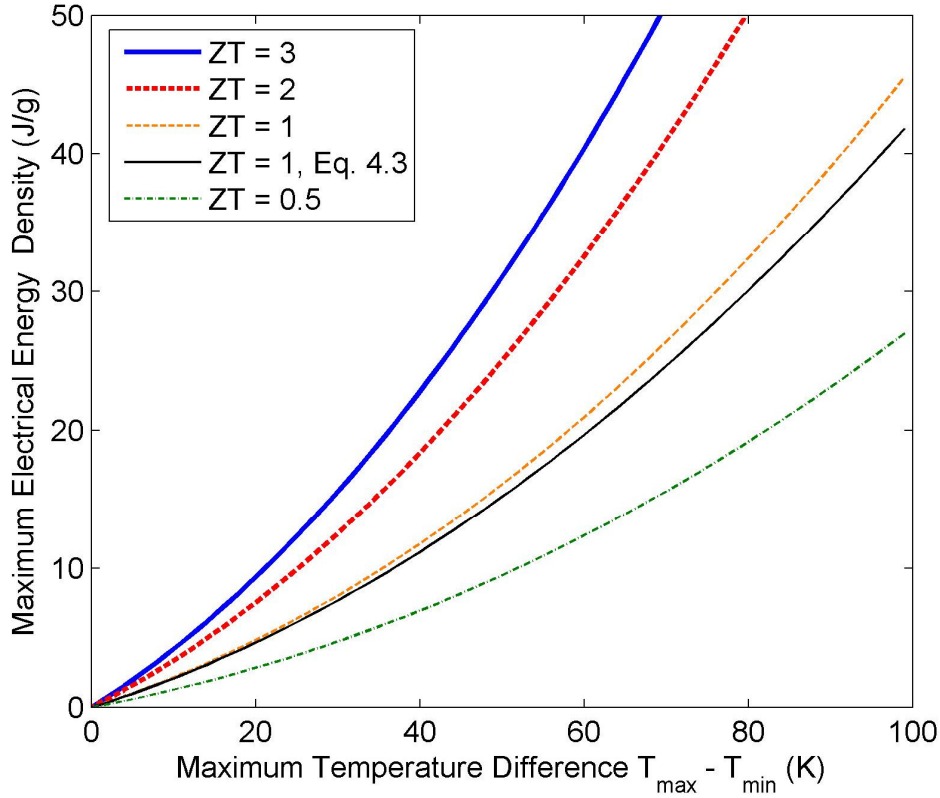


Figure 4: Electrical energy per PCM mass versus ambient temperature variation for TEGs with various ZT values.

5. Design considerations

In this section, the static as well as the dynamic thermoelectric harvesting design rules as introduced in [13] are summarized.

For designing a static harvester, and using commercially available heat sinks, an equation which relates the temperature difference obtained on the thermoelectric module comparing and the temperature applied on system with thermal resistance and the figure of merit is written as [15],

$$\frac{\Delta T_{TEG}}{\Delta T} = \frac{\mathfrak{R}_{TEG}}{2 \left(1 + Z \frac{(T_h + T_c)}{2} \right) (\mathfrak{R}_h + \mathfrak{R}_c)} \quad (6.1)$$

The factor 2 on the equation above shows the limit of what can be achieved with commercially available thermoelectric modules [12]. The thermal resistances of commercially available heat exchangers depending on the convection type are portrayed on

Table 2.

		Convection type	Thermal Resistance (W/K)		
Complexity	↓	Natural	0.5 ... 2.0	↑	Thermal Resistance
		Forced	0.02 ... 0.5		
		Liquid	0.005 ... 0.02		

Table 2: Thermal resistance for different convection types . These thermal resistances reflect to the values which can be achieved by heat sinking structures, and should be taken into account when designing a static harvester [15].

In order to design a dynamic thermoelectric harvesting device for a particular application, a number of key parameters must be considered. The nature of the application will determine the temperature cycle characteristics, namely the temperature range, rate of change and cycle period.

For the selection of a phase change material, phase change within the available temperature range must be ensured. Maximum heat capacity c_p and latent heat with an abrupt phase change are desirable. High thermal conductivity k is required to minimize temperature gradients within the PCM. Additives to enhance k or thermal bridge structures may be used for k enhancement. .

The HSU structure must provide good thermal contact between PCM and TEG while providing good thermal insulation at non-TEG heat paths. Minimization of the HSU surface area that is not covered by TEGs, and the use of highly insulating materials such as polyurethane foam or polystyrene, is required. Depending on the temperature profile of a particular application, control of super-cooling and non-uniform phase changes may also be desirable.

Lastly, a TEG with high thermal resistance is desirable in order to increase the thermal time constant of the system and delay heat flow, such that the maximum possible ΔT is achieved. This is also important for minimization of ΔT loss in the PCM. As it will be explained in detail in section 7, this is in contrast to the static thermoelectric harvesting case where heat resistance matching is required for maximum power harvesting. However, the TEG thermal resistance should be substantially smaller than that of the insulation used, to minimize the heat leakage, and also small enough to ensure a complete phase change cycle within the application-given temperature cycle period. These considerations are important both for the choice of materials and the design of geometry of a dynamic thermoelectric harvester. The desirable characteristics of each constituent part of the device are summarized in

Table 3.

DESIRABLE CHARACTERISTICS	Phase Change Material	Heat Storage Unit	Thermo-Electric Generator
	High heat capacity c_p High latent heat E_{PC} Phase change within temperature range High thermal conductivity Minimised super-cooling	Low thermal resistance of PCM – TEG interface Low <i>thermal resistance</i> insulation Low insulation area to TEG area ratio Thermal bridge for k_{PCM} enhancement	High efficiency at low ΔT $k_{TEG} \ll k_{PCM}, k_{Heat\ Contacts}$ $k_{TEG} \gg k_{HSU\ insulation}$ k_{TEG} small, to maximise T_{PCM} delay k_{TEG} high enough for full phase change

Table 3: Desirable characteristics used to design a heat storage thermoelectric harvester. In this table, k generally represents thermal conductivity.

6. Applications

Thermoelectric energy harvesting has shown great potential on different application scenarios. Depending on the environmental conditions, heat dissipation and sensor requirements, the static or the dynamic energy harvesting approach can be applied in order to build energy autonomous sensor systems. In this section, three different implementations are summarized: a static thermoelectric harvester for aircraft seat sensors, the first dynamic thermoelectric harvesting prototype and a recently reported dynamic device designed for powering aircraft structural monitoring sensor nodes.

6.1. Static thermoelectric harvester for aircraft seat sensors

In this application, wireless monitoring of aircraft seats is desirable, mostly for acquisition of seat state information such as occupancy, tray position, seatbelt status etc. [16] The heat dissipation from the human body (around 100 W in total, [17]) is used as the power source. The equilibrium body-to-seat temperature difference achieved is around 6 K. By matching the heat sink thermal resistance to that of the TEG, a steady-state temperature difference of 3 K across a 10×10 mm TEG with thermal resistance of around 20 K/W was achieved. The TEG was an Eureka TEG1-9.1-9.9-0.8/200. An electrical power output of 0.17 mW was demonstrated, and six such devices were used to achieve the 1 mW goal of the sensor application scenario. A custom power management unit was used for regulating the output voltage at 2.7 V or 3.3 V from an input voltage 0.2 - 0.5 V, in order to operate the microcontroller (MSP430), the RF transceiver (Texas Instruments CC2420) and the sensors (a belt sensor, a tray sensor and right up position of the passenger seat sensor). An infrared image and the installed system are shown in Figure 5. Further information for this implementation may be found in [16]. Different sensors can be powered by energy harvesting and an overall profit on the aviation infrastructure could be established.

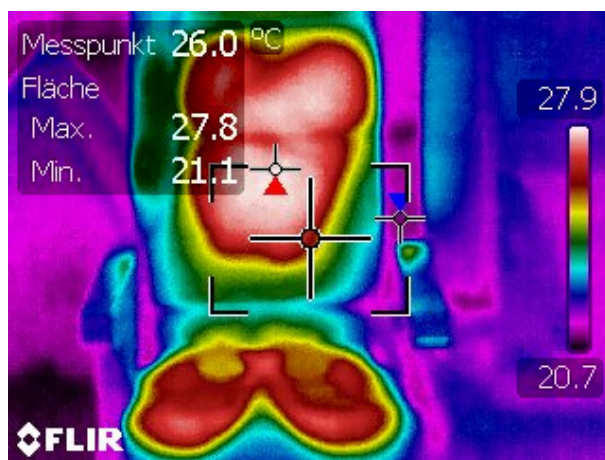


Figure 5: Infrared image (left) and installed demonstrator (right) of a static thermoelectric harvester for aircraft seat sensors [16].

6.2. The dynamic thermoelectric harvesting prototype

A dynamic thermoelectric harvester prototype was developed by EADS Innovation works in 2009 [18]. This prototype consisted of a hemi-spherical stainless steel heat storage unit with an internal thermal bridge, water as the PCM and four EURECA TEG1-9.1-9.9-0.2_200 TEGs. A schematic and image of this implementation are shown in Figure 6. A polyurethane layer was used for thermal insulation. A total output energy of 35 J from an outside temperature sweep corresponding to a typical flight, using 10 ml of PCM was achieved. This device was tested under real flight conditions and for various flight cases demonstrating energy outputs up to 24 J [19]. More information regarding this implementation can be found in [18] and [19]. This prototype was used to power up a wireless sensor node for more than 5 hours, and different sensors ranging from temperature to strain gauge can be adapted and installed in harsh environments.

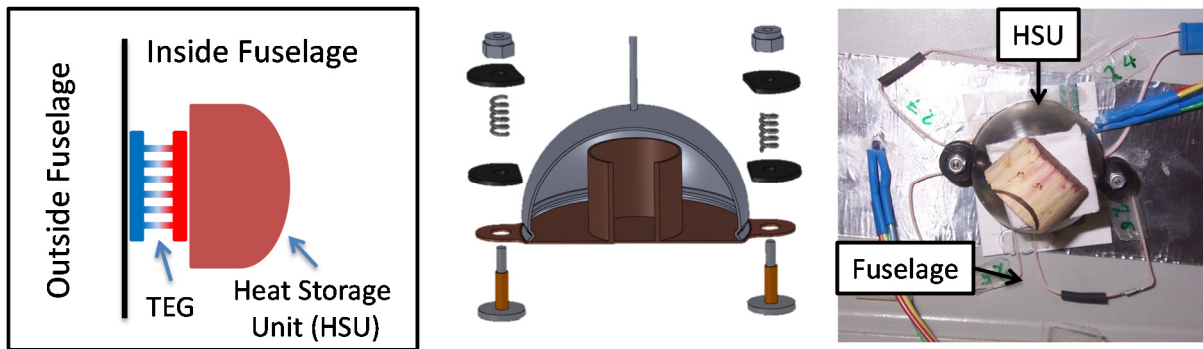
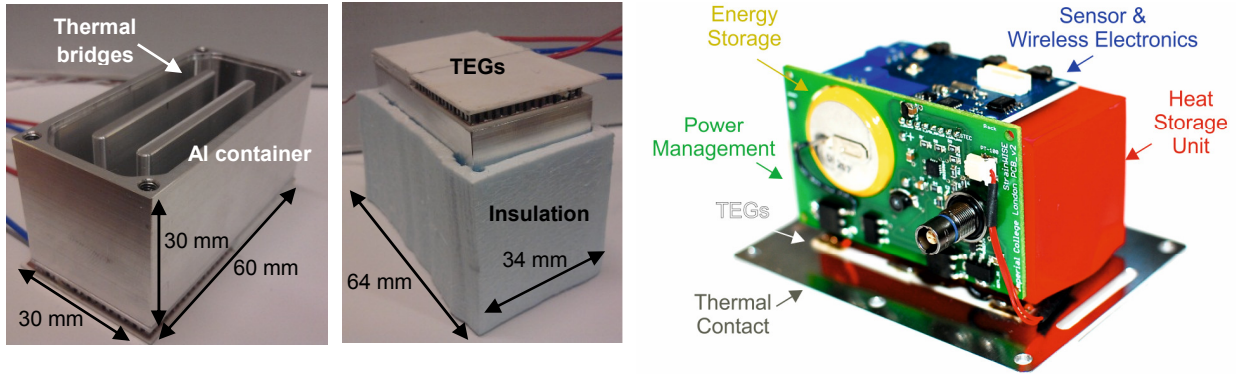


Figure 6: Schematic illustration of the EADS 2008 dynamic harvester implementation from concept to prototype [9].

6.3. Heat storage thermoelectric harvester for aircraft strain sensors

The implementation presented in [13] was based on aluminum HSU with 23 g of water as PCM and a 2 mm thick polystyrene thermal insulation layer. The metal container outer dimensions were $60 \times 30 \times 30$ mm with 2 mm thick walls and included two internal thermal bridges. Its mass was 65 g with an internal volume of 30 cm^3 . Two Marlow TG12-2-5 TEGs were used, each measuring $30 \times 34 \times 4$ mm and thermal resistance 3.6 K/W. The figure of merit ZT , and series resistance of each TEG were 0.72 and 5Ω ($\pm 10\%$) respectively. The main design benefit of this implementation regards the quality of insulation as it doesn't have other heat bridges between the interior and the exterior other than the TEGs, and the extruded polystyrene has an extremely low thermal conductivity ($0.03 \text{ W/m}\cdot\text{K}$). Photographs of the container and the assembled device are shown in Figure 7. Output energy of 105 J into a 10Ω matched resistive load was demonstrated from a temperature sweep from $+20 \text{ }^\circ\text{C}$ to $-21 \text{ }^\circ\text{C}$, then to $+25 \text{ }^\circ\text{C}$. Indicative output power results are shown in Figure 8. This corresponds to an energy-to-PCM volume density of 4.6 J/ml and an energy-to-overall volume density of 1.3 J/ml . Flight tests have been scheduled by Airbus for a strain sensor system powered by this implementation. A photograph of the device is shown in Figure 7 [14].



(a) (b)
 Figure 7: (a) Photographs of the Imperial 2014 dynamic harvester implementation Left: metal container with lid removed, showing the two thermal bridges. Right: assembled generator. The metal container is partially raised for visibility. (b) Photograph of the sensor node (unboxed) [14].

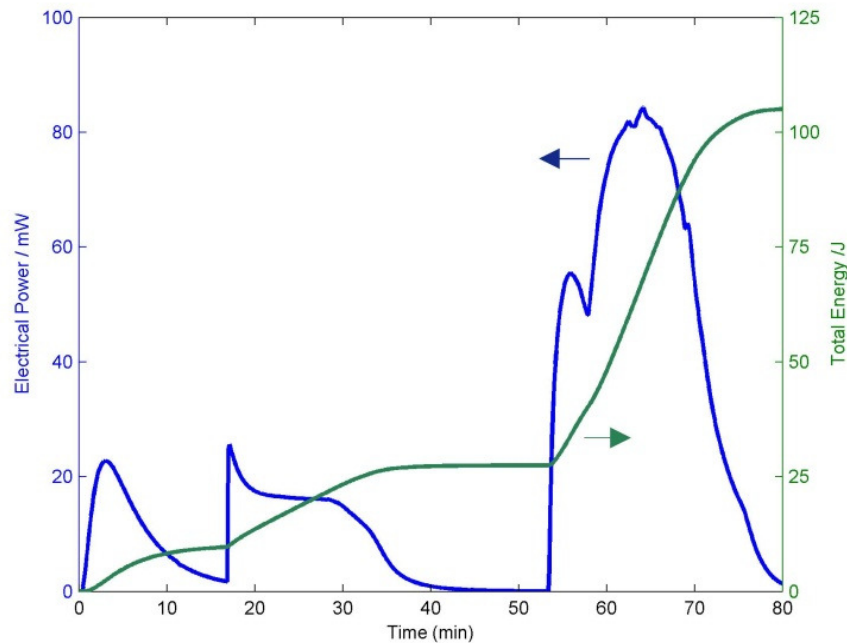


Figure 8: Instantaneous electrical power output and energy of the Imperial 2014 device shown in Figure 7.

6.4. Outlook

While the three application cases described in section 5 are indicative, other implementations have also been reported, such as the dynamic harvester implementation of Baily et al [20] intended for aircraft strain sensors. The reported prototype demonstrated output energy of 34 J from a typical flight temperature cycle. A comparative summary of reported dynamic energy harvesting devices is presented in Table 4.

Organisation/Year	Size/ml	TEG	Energy J	Energy Density J / ml (PCM)	Energy Density J / ml (dev)	Comments
EADS / 2008 [18]	24 plus Insulation	4 x Eureka TEG1-9.1-9.9-0.8/200	35	3.5	1.5 (no insulation)	Flight tested
LAAS-CNRS / 2008 [20]		Micropelt MPGD602	34	2.8		
Imperial / 2014 [21]	78	2 x Marlow TG12-2-5	105	4.6	1.3	Flight tests scheduled

Table 4: Overview of dynamic thermoelectric harvesting device implementations

Overall, both static and dynamic thermoelectric harvesting appear as promising options for powering aircraft sensors. The choice between operation principles and among designs depends on sensor location, size and installation restrictions and power requirements. In parallel with the considerable research on modern thermoelectric devices, such as super-lattice based devices, current research efforts focus on the identification of application scenarios and associated locations. In addition, different PCM materials (salt-based, organic, eutectic etc) are considered in order to expand the applicability of applications [14]. A table with a selection of the commercially available PCMs with their thermal properties is shown in

Table 5.

Finally, the use of multiple PCMs to improve operational continuity of dynamic harvesting is investigated [22]. Due to the large variety of advancement potentials of the devices reviewed here, the development of a device - application combination assessment tool is desirable, to be used as a compass-tool towards future implementations. In this direction, a set of design rules have been proposed in [13] and are outlined in the next section.

The performance of a thermoelectric energy harvesting device hinges, more than on anything else, on the efficiency of the TEG used. Current state of the art TEGs only provide a very small efficiency margin (2-5%) which in turn limits the overall efficiency of the device to $\approx 0.5\%$. Performance figures are even worse for smaller device sizes or small ΔT s. It becomes obvious that more efficient and scalable TEGs are crucial for challenging thermoelectric energy harvesting applications, not only in aircraft but potentially for other application sectors.

Material Name		Physical Properties				
		T_m [°C]	C_p [kJ/kg·K]	k [W/m·K]	ρ [kg/m ³]	ΔH [kJ/kg]
Water (sol.)		0	4.2	2.18	917	334
Water (liq.)			2	0.58	1000	
PCM Inorganic	E-11 (PCM Products)	-11.6	3.55	0.57	1090	301
	E-15 (PCM Products)	-15	3.87	0.53	1060	303
	E-19 (PCM Products)	-18.7	3.29	0.58	1125	282
	H120 (PCM Products)	120	1.51	0.506	2220	120
	H355 (PCM Products)	353	1.52	0.556	2060	230
PCM Organic	RT10-HCG (Rubitherm)	+10 – +9	2	>0.2	770	152
	RT10-HC (Rubitherm)	+10 – +4	2	0.2	770	195
	RT-9-HCG (Rubitherm)	-9 – -10	2	>0.2	770	260
	A118 (PCM Products)	118	2.7	nd	1450	340

Table 5: Physical properties of the most used phase change materials for thermoelectric applications. In brackets the manufacturer of each PCM is given. On the “normal” temperature range (-50°C to 80°C) water has one of the best thermal properties.

7. Conclusions

The development of reliable and adaptable energy harvesting solutions is critical for the success of autonomous, wireless sensor nodes. A successful example can be found in the dynamic thermoelectric harvesting sensors which have recently been demonstrated in real flight environments, showing that harvesting can provide enough energy to power sensors and wireless transceivers for an adequate amount of time [19].

In comparison with conventional, also referred to in this chapter as static, thermoelectric harvesters, optimization of performance has a critical difference. As discussed in section 4.2, in cases where a TEG is used to exploit a local temperature difference directly, the energy source can typically be approximated as a limitless supply of heat at constant temperature, with the input temperature to the TEG affected only by the finite thermal conductance of the source structure, not by the loss of energy through the TEG. Consequently, maximization of energy output requires maximization of the product of heat flow and TEG efficiency as shown in Figure 9 (a). Taking under consideration the approximately linear variation of η_{TEG} with ΔT , simple calculations show that the TEG thermal resistance should match that of the rest of the thermal path between the high temperature source and the ambient. This is why optimum operation in direct thermoelectric harvesters occurs when the temperature difference across the TEG is $\Delta T/2$, in analogy with load matching in electrical power transfer.

On the contrary, in heat storage thermoelectric harvesting, the total available heat energy is limited, and hence maximization of conversion efficiency, rather than output power, is required. By virtue of that, a TEG with as large a thermal resistance as possible is desirable. An electrical analogy of this effect can be found in the discharge of a capacitor into a resistive load, through its own series resistance, as shown in Figure 9 (b). As opposed to the case of power transfer from a voltage source where resistance matching is required, in the case of a capacitor discharge, maximization of the load resistance is required.

The theoretical background, the design considerations and the implemented prototypes illustrate the great potential of thermoelectric energy harvesting deployed in aircraft wireless sensor networks. Harsh environments or difficult to access areas can be monitored using thermoelectric harvesters as supply sources. These sources may reduce maintenance costs, weight and hence reduce fuel consumption, and finally operational costs.

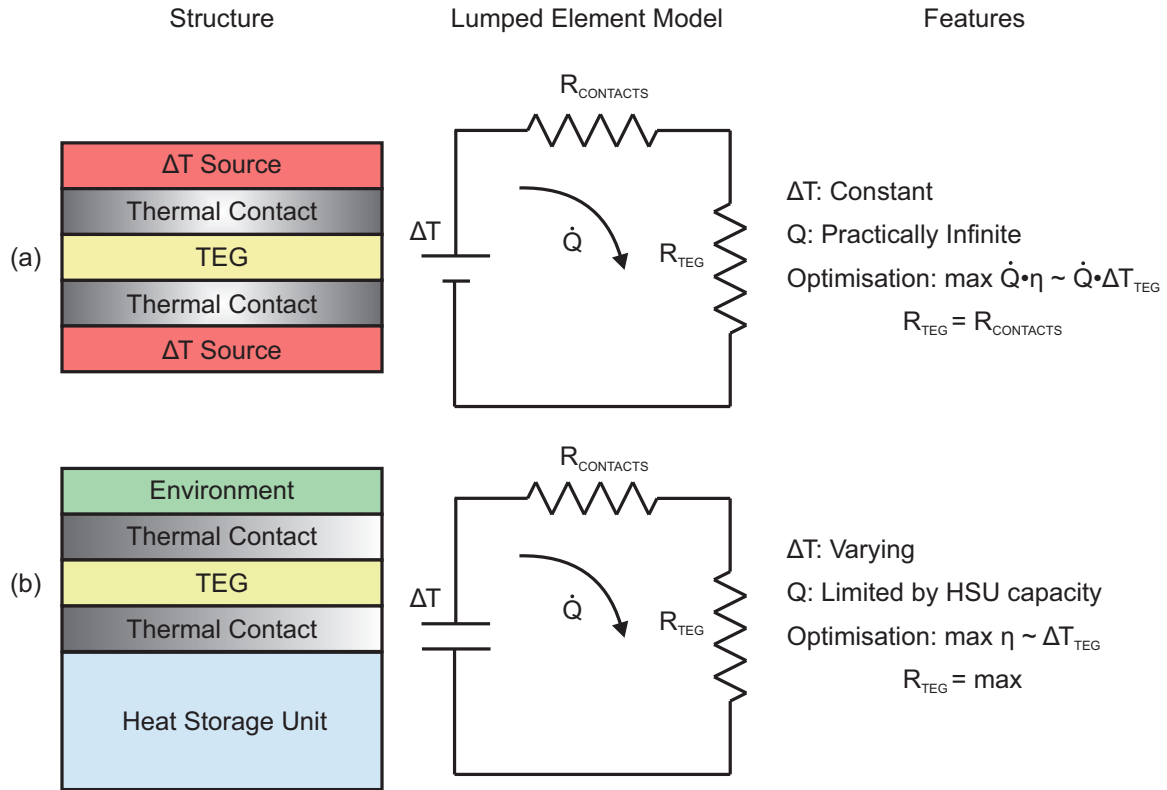


Figure 9: (a) Direct thermoelectric harvesting. Heat availability is practically unlimited and optimum operation requires thermal resistance matching. (b) Heat storage thermoelectric harvesting architecture. Maximum thermal resistance is required.

8. Works Cited/References

- [1] P. Kowalewski, Cost-Benefit-Analysis of Wireless Sensor Networks and Energy Harvesting. Master Thesis, Fachhochschule Wedel, 2012.
- [2] C. González and J. Homero, Conduction of Profitability Analyses in Research and Development Projects. Master Thesis, Technical University of Hamburg, 2013.
- [3] T. Becker, M. Kluge, J. Schalk, K. Tiplady, C. Paget, U. Hilleringmann and T. Otterpohl, "Autonomous sensor nodes for aircraft structural health monitoring. *Sensors Journal*", IEEE, 9(11), 1589-1595, 2009.
- [4] A. S Weddell, G. V. Merrett, and B. M. Al-Hashimi, (2011, March). Ultra low-power photovoltaic MPPT technique for indoor and outdoor wireless sensor nodes. In Design, Automation & Test in Europe Conference & Exhibition (DATE), 2011 (pp. 1-4). IEEE.
- [5] K. Thangaraj, A. Elefsiniotis, T. Becker, U. Schmid, J. Lees, C. A. Featherston and R. Pullin, "Energy storage options for wireless sensors powered by aircraft specific thermoelectric energy harvester". *Journal of Microsystem Technologies*, DOI: 10.1007/s00542-013-2009-3, 2013.
- [6] M. T. Penella, and M. Gasulla, "Runtime extension of low-power wireless sensor nodes using hybrid-storage units", *Instrumentation and Measurement, IEEE Transactions on*, 59(4), 857-865, 2010.
- [7] Report ITU-R M.2197, "Technical characteristics and operational objectives for wireless avionics intra-communications (WAIC)", ITU 2011.
- [8] G. J. Snyder and E.S. Toberer, "Complex thermoelectric materials", *Nature materials*, 7(2), 105-114, 2008.
- [9] M. Strasser, R. Aigner, M. Franosch and G. Wachutka, "Miniaturized thermoelectric generators based on poly-Si and poly-SiGe surface micromachining", *Sensors and Actuators A: Physical*, 97, 535-542, 2002.
- [10] D. M. Rowe and CRC Handbook of Thermoelectrics: CRC Press, 1995.
- [11] M. Freunek, M. Müller, T. Ungan, W. Walker and L. M. Reindl, "New physical model for thermoelectric generators", *Journal of electronic materials*, 38(7), 1214-1220, 2009.
- [12] G. Min and N. M. Yatim, Variable thermal resistor based on self-powered Peltier effect. *J. Phys. D: Appl. Phys.*, 41(222001), 222001, 2008.
- [13] M. E. Kiziroglou, S. W. Wright, T. T. Toh, P. D. Mitcheson, T. Becker, and E. M. Yeatman, "Design and Fabrication of Heat Storage Thermoelectric Harvesting Devices," *Industrial Electronics, IEEE Transactions on*, vol. 61, pp. 302-309, 2014.
- [14] M. E. Kiziroglou, A. Elefsiniotis, S. W. Wright, T. T. Toh, P. D. Mitcheson, T. Becker, and E. M. Yeatman, "Performance of phase change materials for heat storage thermoelectric harvesting," *Applied Physics Letters*, vol. 103, pp. 193902-193902-5, 2013.
- [15] S. Beeby and N. M. White, *Energy harvesting for autonomous systems*. Artech House, 2010.
- [16] D. Samson, M. Kluge, T. Becker and U. Schmid, "Energy Harvesting for Remote Monitoring of Aircraft Seats", *Sensor Letters*, 8(2), 328-335, 2010.
- [17] T. Starner. "Human-powered wearable computing." *IBM systems Journal* 35, no. 3.4 (1996): 618-629.

- [18] D. Samson, T. Otterpohl, M. Kluge, U. Schmid and Th. Becker, Aircraft-Specific Thermoelectric Generator Module. *Journal of Electronic Materials*, 39(9), pp. 2092-2095, 2009.
- [19] A. Elefsiniotis, D. Samson, T. Becker and U. Schmid, "Investigation of the Performance of Thermoelectric Energy Harvesters Under Real Flight Conditions", *Journal of Electronic Materials*, 42(7), pp.2301-2305, 2013.
- [20] N. Baily, J. M. Dilhac, C. Escriba, C. Vanhecke, N. Mauran, M. Bafleur, "Energy scavenging based on transient thermal gradients: Application to structural health monitoring of aircrafts", *Conf. Proceedings of PowerMEMs 2008*, Sendai, Japan, 2008.
- [21] T. T. Toh, S. W. Wright, M. E. Kiziroglou, P. D. Mitcheson and E. M. Yeatman, "A Dual Polarity, Cold-Starting Interface Circuit for Heat Storage Energy Harvesters", *Sensors and Actuators A*, accepted, 2014
- [22] A. Elefsiniotis, N. Kokorakis, T. Becker and U. Schmid, "A thermoelectric-based energy harvesting module with extended operational temperature range for powering autonomous wireless sensor nodes in aircraft." *Sensors and Actuators A: Physical*, vol. 206, pp. 159-164, 2013.